Crystal Structure and Packing Disorder of Poly(*p*-phenylenebenzobisoxazole): Structural Analysis by an Organized Combination of X-ray Imaging Plate System and Computer Simulation Technique

Kohji Tashiro,*,† Junichi Yoshino,† Tooru Kitagawa,‡ Hiroki Murase,‡ and Kazuyuki Yabuki‡

Department of Macromolecular Science, Graduate School of Science, Osaka University, Toyonaka, Osaka 560-0043, Japan, and Research Center, Toyobo Co. Ltd., Katata, Ohtsu, Shiga 520-02, Japan

Received January 28, 1998; Revised Manuscript Received May 11, 1998

ABSTRACT: To clarify the crystal structure of poly(*p*-phenylenebenzobisoxazole) (PBO) fibers, the analysis has been made for the X-ray diffraction data collected by the imaging plate system in combination with the computer simulation technique. The characteristic features of the X-ray diffraction pattern of PBO fiber are seen in the spotlike equatorial reflections and the diffuse reflections along the layer lines. The peak positions of the diffuse layer−line reflections were found to fit well to those of the molecular transform calculated for a uniaxially oriented isolated chain, suggesting an appreciably low correlation in the relative height between the neighboring chains. Among many types of the energetically minimized crystal structural models constructed by a computer simulation technique, a model giving a good fit between the observed and calculated X-ray profiles was found, in which the chains are assumed to form the layers extending along the 110 planes with the relative heights of the adjacent chains in the sheets almost confined to either $+c/4$ or $-c/4$ (c = fiber identity period) and these sheets are stacked together in the *b*-axis direction with random heights along the chain axis.

Introduction

Poly(*p*-phenylenebenzobisoxazole) (PBO) has been attracting much attention because of its excellent mechanical properties.[1−12] Among many kinds of fibers,

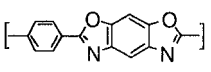

PBO

PBO shows the highest Young's modulus along the chain axis. The modulus of the bulk PBO samples is being improved at this time to approach the ultimate modulus or crystallite modulus of this polymer, which was evaluated as 477[13] or 478[14] GPa by the X-ray diffraction method and as 460 GPa by the lattice dynamical calculation[15] (the theoretical value 690 GPa was also reported by semiempirical molecular orbital calculation, but this seems to be overestimated as pointed out by the authors themselves[16]).

The morphological study of PBO fibers has been reported in many papers (for example, refer to refs 17−30). To clarify the intimate relationship between structure and mechanical properties of the PBO fiber, the detailed information on the crystal structure is essentially important. So far, several research groups[31−33] proposed the crystal structure of PBO on the basis of the X-ray and electron diffraction data. However, the proposed structures could not necessarily reproduce the whole X-ray diffraction pattern reasonably. For example, Fratini et al.[32] proposed the crystal structure of PBO with an X-ray reliability factor of 11.4%. Their structural model can reproduce the observed equatorial reflection intensity well, but the agreement in the layer−line reflections is not very good between the observed and calculated results. This disagreement seems to be related with the characteristic layer−line profiles of PBO fibers or the diffuse-scattering-type profiles, making it difficult to evaluate the structure factors. We need to reproduce the whole patterns of layer reflections (1-dimensional and 2-dimensional) as well as the peak intensities. Modifying the structure of Fratini et al., Martin and Thomas proposed the new structure.[33] The two chains are packed in the monoclinic unit cell of the parameters $a = 11.20$ Å, $b = 3.54$ Å, c (fiber axis) = 12.05 Å, and $\gamma = 101.3°$. The space groups described by them is *Pc* (No. 7; exactly speaking, it should be *Pa*) and the neighboring chains are shifted by $c/4$ along the chain axis. This axial shift of chains is made by $+c/4$ or $-c/4$ randomly along the *a* axis. Their structural model seems essentially correct, but they gave the predicted diffraction pattern only qualitatively and schematically and they did not calculate the structure factors of the possible reflections so as to compare them with the observed data in a quantitative manner. The structural investigations based on the molecular mechanics calculation or the molecular orbital calculation were also reported by several people[34−40] in order to find out the energetically stable molecular conformation of PBO chain, but no trial was made to check the reasonableness of their models through the quantitative evaluation of the X-ray diffraction pattern.

Recently we have developed a new system[41−43] to analyze the structure of polymer crystals on the basis of an organized combination of X-ray diffraction, electron diffraction, infrared and Raman spectroscopy, and computer simulation techniques. By using this system,

† Osaka University.
‡ Toyobo Co. Ltd.

S0024-9297(98)00113-2 CCC: $15.00
Published on Web 07/21/1998

we analyzed the crystal structure of the model compound of PBO, the structural parameters of which might be utilized for the modeling of the PBO chain conformation necessary for the structure analysis of the PBO crystal.[44,45] But, even when the geometrically reasonable chain structure could be obtained, the packing structure of these chains must be clarified. As mentioned above, this polymer shows the characteristic X-ray diffraction pattern, in which the equatorial reflections are spotlike but the layer lines exhibit remarkable streaking. This requires us to introduce a disorder into the crystal structure so as to succeed in a quantitative reproduction of the X-ray diffraction patterns, as already pointed out by several groups. For example, Suehiro et al.[47] analyzed the streaking X-ray diffraction pattern of poly(β-propiolactone) on the basis of the paracrystalline theory. Granier et al.[46] interpreted the characteristically streaking electron diffraction pattern of poly(*p*-phenylenevinylene) by introduction of the translational disorder along the chain axis on the basis of paracrystalline theory. The analytical calculation of the X-ray diffraction pattern by using such a paracrystalline theory is one useful method. As another useful method, we can consider the computer simulation technique, where the concrete crystal lattice model consisted of many chains is built up and the position and/or orientation of these polymer chains is disordered following a predetermined rule, and then the X-ray diffraction patterns are calculated and modified by changing the structure by a suitable method. In the present paper we measured the X-ray fiber diagram of the highly oriented PBO fibers by using an X-ray imaging plate, and the data were transferred to a computer in a digitized form. Then the characteristic X-ray diffraction pattern of the PBO fibers was simulated by constructing the concrete crystal lattice models in which many number of PBO chains were packed in a systematic or nonsystematic way with respect to the relative height along the chain axis.

Experimental Section

Samples. PBO fibers were spun from polyphosphoric acid solution and annealed at ca. 600 °C. The Young's modulus of the fiber was ca. 350 GPa. The observed density was 1.56 g/cm^3.

X-ray Measurements. The X-ray diffraction diagram of PBO was taken by using an imaging plate system DIP3000 with a cylindrical camera of radius 149.7 mm (MAC Science, Co. Ltd., Japan). The X-ray generator was a SRA18X (MAC Science Co. Ltd.) and the electric power was 50 kV and 200 mA. The Mo Kα line was used as an X-ray source in order to collect as many reflections as possible. To avoid the heterogeneity of reflection intensities coming from the bundling of fibers, the sample was oscillated in the range of ca. 50° around the fiber axis (a full rotation could not be made because of the geometrical limitation coming from the metal holder keeping the fibers straight). The total measurement time was 400 min. The thus-measured X-ray fiber diagram of PBO is reproduced in Figure 1. The X-ray profiles of the equatorial and layer lines were obtained by integrating the reflection intensities along each layer line over a proper width. This integration was performed by utilizing a software (XPRESS) supplied by MAC Science Co. Ltd. Among the thus-calculated profiles, the first line profile is not shown here since the strong and broad reflections on the equatorial line overlap partly the first line reflections, making it difficult to carry out the exact integration.

Computer Simulation. Modeling of PBO crystal structure and simulation of the X-ray diffraction pattern were carried out by using a commercially available software Cerius^2 (Version 2.0, Molecular Simulations Inc.). The energy minimization of the structural models was made on the basis of the "Dreiding II" force field.[48] The point charges were assigned to each atom by the method proposed by Gasteiger.[49] Although these potential force field and atomic charges might not be suitable to this PBO case, we used these parameters tentatively and the energy minimization was made in order to avoid the stereochemically unreasonable chain packings. If we need to calculate the physical properties, for example, more quantitatively and exactly, the force field parameters must be refined thoroughly. The refinement can be made effectively by using not only the X-ray data but also the vibrational spectroscopic data and is now being performed by our other group.

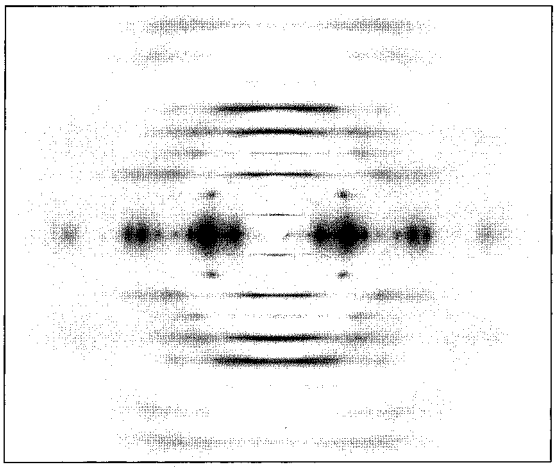

Figure 1. X-ray diagram observed for PBO fiber. The fiber axis is vertical. The X-ray beam is the Mo Kα line.

The calculation of the one-dimensional and two-dimensional X-ray diffraction patterns of the models was made by utilizing a software installed in the program Cerius^2. In the calculation, the following parameters were employed concerning the shape of crystallite, the degree of chain orientation, temperature factor and so on: the crystallite size, $L_a = 220$ Å, $L_b = 180$ Å, and $L_c = 300$ Å; the lattice strain, $\epsilon_a = 0.5\%$, $\epsilon_b = 1.0\%$, and $\epsilon_c = 0.5\%$; the isotropic temperature factor, $B_{iso} = 3.0$ Å^2; degree of chain orientation = 1.5°. These parameters were determined not experimentally but by a trial-and-error method so that the calculated profiles were fitted to the observed data as well as possible. The experimental determination of these parameters will be made in the near future to check the values used above.

Results and Discussion

I. Determination of Cell Parameters. As shown in Figure 1, the equatorial reflections are spotlike. In total the 11 Bragg reflections were identified definitely. The second layer line reflections are relatively sharp but most of the other layer lines are diffuse. On the basis of the software developed by our group,[41] indexing of the observed reflections was made. The thus determined cell parameters are of monoclinic type with $a =$ 11.15 Å, $b = 3.60$ Å, c (fiber axis) = 12.13(5) Å, and $\gamma =$ 100.0°. The space group is $P11a$-C_s^2. This unit cell is very similar to that proposed by Fratini et al.[32] Judging from the diffuse scattering along the layer−lines, PBO is considered to have some packing disorder in the crystal lattice as already pointed out in many papers. Therefore the thus determined unit cell parameters should be assumed to be an "averaged" or "basic" cell necessary for the discussion of the packing structure, as will be described below in more detail.

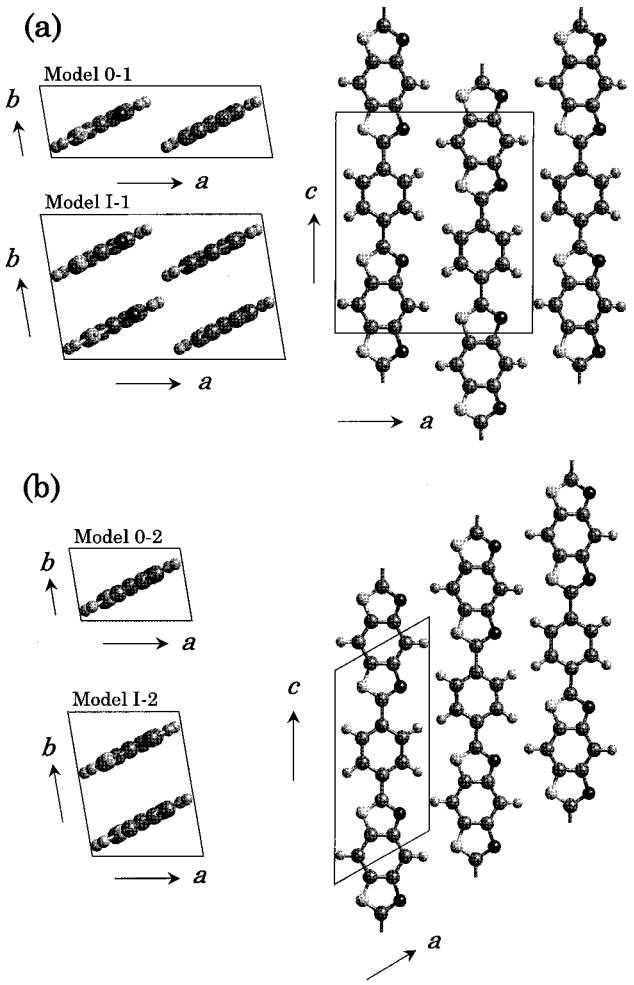

Figure 2. Initial structure models of PBO crystal. (a) The adjacent chains along the *a* axis is shifted by $+c/4$ and $-c/4$ alternately. The number of chains included in the basic unit cell is 2 in model 0-1 and 4 in model I-1. In the latter case the relative height of chains along the *b* axis is shifted by $c/2$. (b) The adjacent chains along the *a* axis are shifted by $+c/4$. The number of chains included in the basic unit cell is 1 in model 0-2 and 2 in model I-2. In the latter case the relative height of chains along the *b* axis is shifted by $c/2$.

II. Simulation of X-ray Fiber Diagram. Construction of Starting Models. If the observed density and the unit cell parameters determined above are taken into consideration, the two PBO chains were assumed to be contained in the basic unit cell. Different from the chain structures proposed by Fratini et al.,[32] in our models the torsional angle between the benzene ring and heterocyclic ring is almost coplanar, which is consistent with that seen for the low molecular weight model compounds of PBO as clarified by the X-ray structural analysis.[44,45] This coplanar form is energetically stable. In the following sections there should appear many types of models, but the chain conformation is almost the same even after the energy minimization of these models.

These two chains were rotated and translated freely so that the observed diffraction data could be reproduced as well as possible. As a result, the two types of crystal structure shown in parts a and b of Figure 2 were obtained as candidates used for the more detailed simulation. These models will be called model 0-1 and model 0-2, respectively. In model 0-1 of Figure 2a, the relative height of the adjacent chains is shifted by $+0.25c$ and $-0.25c$ alternately along the *a* axis. In model 0-2 the basic unit cell is just a half that of model 0-1 and only one chain is included in this triclinic type cell. The cell parameters are changed to $a = 6.35$ Å, $b = 3.60$ Å, c (fiber axis) $= 12.13$ Å, $\beta = 61.46°$ and $\gamma = 98.77°$. The adjacent chains along the *a* axis are shifted by the same pitch ($+0.25c$) in the same direction of the chain axis. The shift of $\pm 0.25c$ between the adjacent chains is different from the value of $0.1c$ reported by Fratini et al.[32] After constructing these models, we happened to notice that our structural model is essentially the same as that proposed by Martin and Thomas[33] with respect to the relative height of the chains at least. Table 1 shows the fractional coordinates of the constituent atoms in the model 0-1.

Table 1. Fractional Coordinates of the Constituent Atoms of the PBO Crystal (Model 0-1)[a]

atom[b]	*x*/*a*	*y*/*b*	z/c
C1	0.189	0.382	0.230
C2	0.122	0.286	0.133
C3	0.186	0.379	0.035
C4	0.306	0.552	0.033
C5	0.373	0.647	0.130
C6	0.309	0.555	0.228
H7	0.027	0.150	0.135
H8	0.467	0.783	0.129
N9	0.145	0.322	0.926
N10	0.143	0.328	0.334
O11	0.344	0.608	0.925
O12	0.342	0.614	0.329
C13	0.246	0.467	0.866
C14	0.245	0.475	0.391
C15	0.247	0.469	0.744
C16	0.353	0.623	0.686
C17	0.355	0.626	0.571
C18	0.250	0.476	0.512
C19	0.143	0.322	0.568
C20	0.141	0.318	0.683
H21	0.435	0.740	0.731
H22	0.437	0.745	0.527
H23	0.062	0.205	0.522
H24	0.058	0.198	0.726

[a] The unit cell parameters of model 0-1 are $a = 11.15$ Å, $b = 3.60$ Å, c (fiber axis) $= 12.13(5)$ Å, and $\gamma = 100.0°$. [b] The numbering of the atoms is shown in the following illustration:

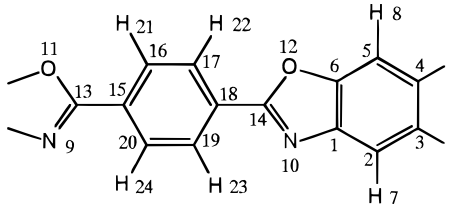

Figure 3 shows the comparison of the observed X-ray reflection profiles with those calculated for model 0-1. Figure 4 (a) shows the calculated fiber diagram for model 0-1. Model 0-2 gave almost the same calculated results as model 0-1, and so the data were not shown here. As seen in Figures 3 and 4, these two models, 0-1 and 0-2, gave relatively good correspondence between the observed and calculated X-ray peak positions for equatorial reflections but could not reproduce the layer line profiles well.

To get another structure possibility, the repeating unit cells of models 0-1 and 0-2 were expanded twice along the *b* axes and the four chains (in model 0-1) or too chains (in model 0-2) were packed in these larger cells. After a trial-and-error process, we found new models, the packing energies of which were not so much

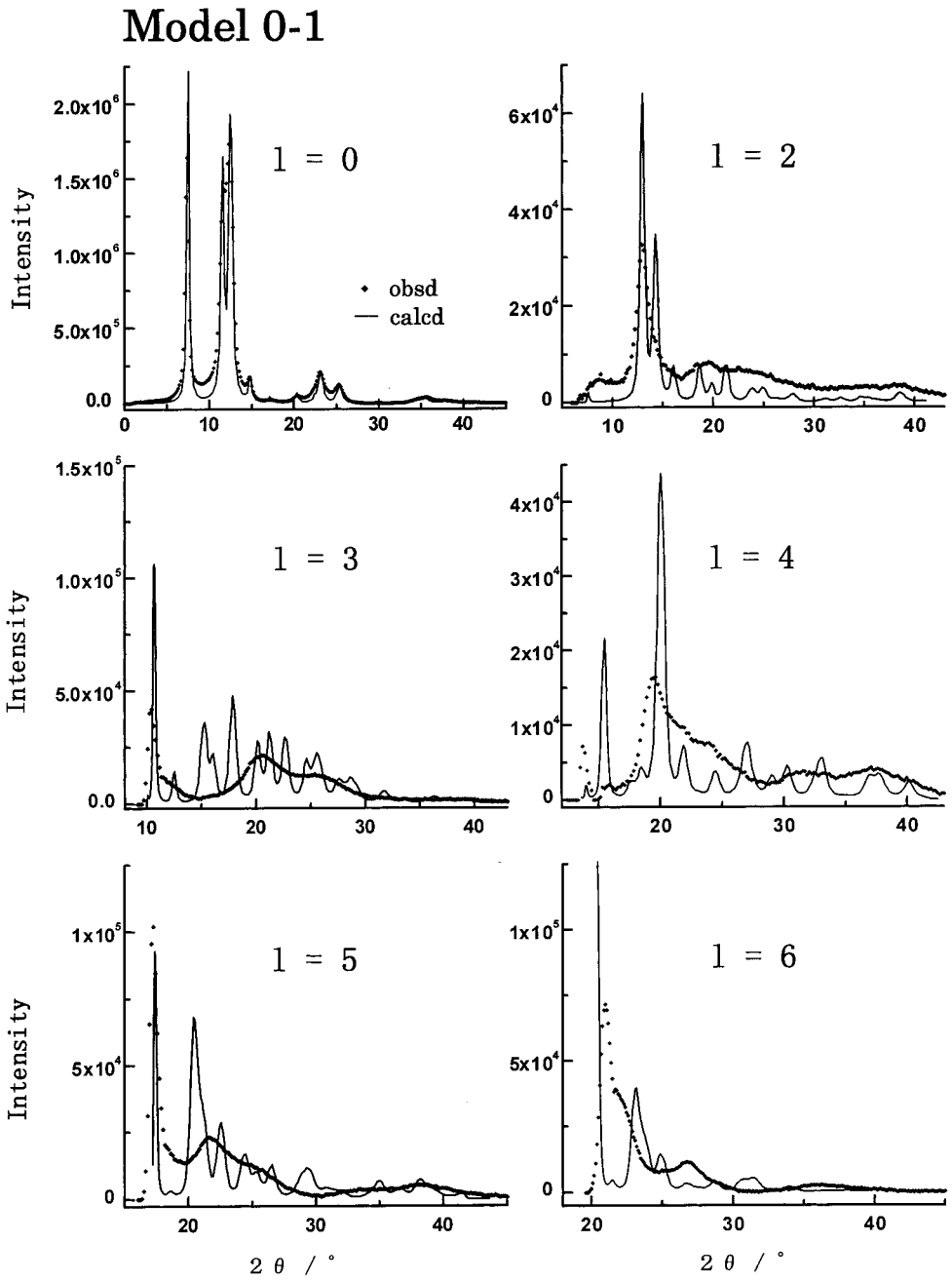

Figure 3. Comparison of the observed X-ray reflectional profiles (·) of PBO fiber with those calculated for the model 0-1 (Figure 2) as indicated by solid lines. The profile of the first layer line is not shown here because the equatorial reflections of large size disturb the exact integration of the first layer line reflections. The used X-ray beam is the Mo Kα line.

different from those of the original models 0-1 and 0-2. These new models are called model I-1 and model I-2, respectively, as shown in parts a and b of Figure 2, where the newly added couple of chains along the *b* axes were shifted by 0.5*c* from the height of the original couple of chains. The calculated energies of these lattices are as follows.

model 0-1 54.94 kcal/mol monomeric unit

model I-1 55.20 kcal/mol monomeric unit

model 0-2 54.70 kcal/mol monomeric unit

model I-2 55.19 kcal/mol monomeric unit

The X-ray profiles were calculated for these two models I-1 and I-2. For example, Figure 4b shows the 2-dimensional fiber diagram calculated for model I-1. Similarly to models 0-1 and 0-2, these models were found to give a good result for the equatorial line profile but could not reproduce the entire profile of the layer lines at all.

Molecular Transform. As mentioned above, all the models 0-1, 0-2, I-1, and I-2 could reproduce the observed profiles of the equatorial line and the peak position of the several layer line reflections, but the profiles of the layer lines could not be reproduced well. Observation of diffuse scatterings of the layer lines allows us to speculate that some disordering might exist in the relative heights of the neighboring chains. One extreme case of this translational disordering is a perfectly random correlation between the neighboring chains. Therefore the calculation of the molecular transform or the calculation of structure factor for an

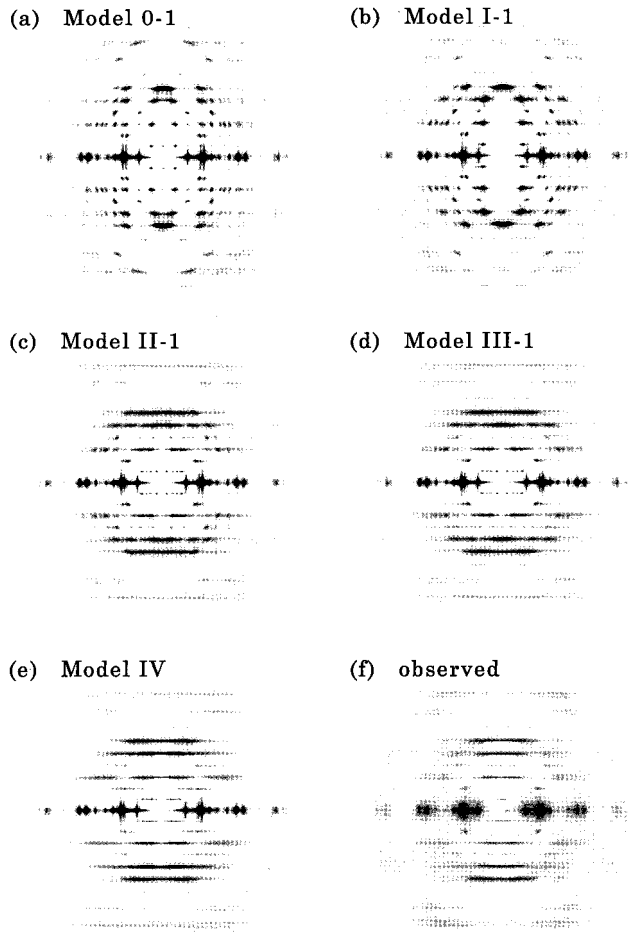

Figure 4. Comparison of the observed X-ray fiber diagram of PBO with the calculated results for the various types of models: (a) model 0-1; (b) model I-1; (c) model II-1; (d) model III-1; (e) model IV; (f) the observed data. The used X-ray beam is the Mo Kα line.

isolated molecular chain might help us to get useful information concerning the translational disordering. Figure 5 shows the results calculated for a uniaxially rotated PBO chain constructed of 16 monomeric units. The calculated layer line profiles were found to show relatively good correspondence to the observed data. That is to say, we should introduce an appreciably large translational disorder along the chain axis into the crystal structure of PBO.

Disorder Models. In the numerical calculation of the diffraction patterns for the models with disordered chain packing structure, the models should be as large as possible. As the first trial, we constructed a structure in which the basic unit cell (model I-1) was enlarged by 4 times along the *a* and *b* axes, respectively, or 64 chains in total were contained in this large cell. There are, of course, infinitely many ways how to introduce disorder to the original structure models 0-1, 0-2, I-1, and I-2. We have chosen some most-probable types of disorder by referring to the packing character of chains in the cell. These models are named models II (or II-1), III (or III-1), and IV as illustrated in Figure 6, where models II and III are renamed as models II-1 and III-1, respectively, because they originate from model I-1 in Figure 2. The details of these models are described below.

Model II (or II-1). In the computer modeling of the various structures we found that the chains arrayed adjacently along the $1\bar{1}0$ plane with a shift of 0.25c are quite tightly packed, and so this arrangement of chains may be assumed to be one rigid sheet. Therefore the translational disordering is assumed to occur between a series of these sheet planes. As shown in Figure 6a, we introduced the random disordering of the *c*-axial shift of the sheets along the *b* axis, where the magnitude of shift (0−1.0*c*) was determined by generating random numbers.

Model III (III-1). In addition to the slippage-type disorder of the sheets, the relative height of the chains included in a sheet must be also disordered more or less. As shown in Figure 6b, we assumed a series of rows along the *b* axis in the model II and gave the random *c*-axial shift to each row, where the magnitude of the shift was one tenth that given for model II because of the tightness of the sheets as pointed out in the description of model II.

The similar construction of models II-2 and III-2 were made starting from the model I-2 of Figure 2. The structures of these models are not shown here, because the projected structures are the same with those shown in parts a and b of Figure 6.

Model IV. All the 64 chains included in the extended cell were shifted randomly along the chain axis (0−1.0*c*) by generating random numbers (Figure 6c).

To evaluate the degree of disordering of these three models, we introduce here a kind of parameter representing a disordering of the relative height (Z_i) of the adjacent chains

$$\langle \Delta z(x) \rangle = [\sum_i | |Z_i|/c - {}^1/_4 |]/n$$

where Z_i is the *Z* coordinate of a particular atom of the *i*-th chain and is in units of Å. *c* is the value of the basic unit cell (=12.13 Å), and *n* is the total number of chains included in the cell. The notation *x* indicates the direction along which the Δ*z* is calculated. The translational disorder parameter ⟨Δ*z*(x)⟩ calculated for the above-mentioned three models are

	⟨Δ*z*(*a*)⟩	⟨Δ*z*(*b*)⟩	⟨Δ*z*($1\bar{1}0$)⟩
model I-1	0.0	0.25	0.0
model II-1	0.118	0.133	0.0
model II-2	0.118	0.133	0.0
model III-1	0.125	0.125	0.033
model III-2	0.133	0.117	0.033
model IV	0.121	0.131	0.120

The ⟨Δ*z*($1\bar{1}0$)⟩ values of models II-1 and II-2 are 0 because the neighboring chains have a difference in height of *c*/4 along the ($1\bar{1}0$) direction without any disordering in the rigid sheet planes. In models III-1 and III-2, this deviates from 0 because of introduction of slight disordering of the relative height along the ($1\bar{1}0$) plane. The randomly shifted model IV gives the larger value of ⟨Δ*z*($1\bar{1}0$)⟩.

Figure 4 compares the fiber diagrams calculated for models 0-1, I-1, II-1, III-1, and IV with the observed one. As the degree of the *c*-axial translational disorder is increased, the diffuse scattering of the layer lines becomes more remarkable and more similar to the observed diagram. In particular, models III-1 and IV were found to give better agreement with the observed data. Many models with disordering parameters similar to those of the models III-1 and IV were created, the fiber diagrams of which gave still good agreement with the observed diffraction pattern. Similar calcula-

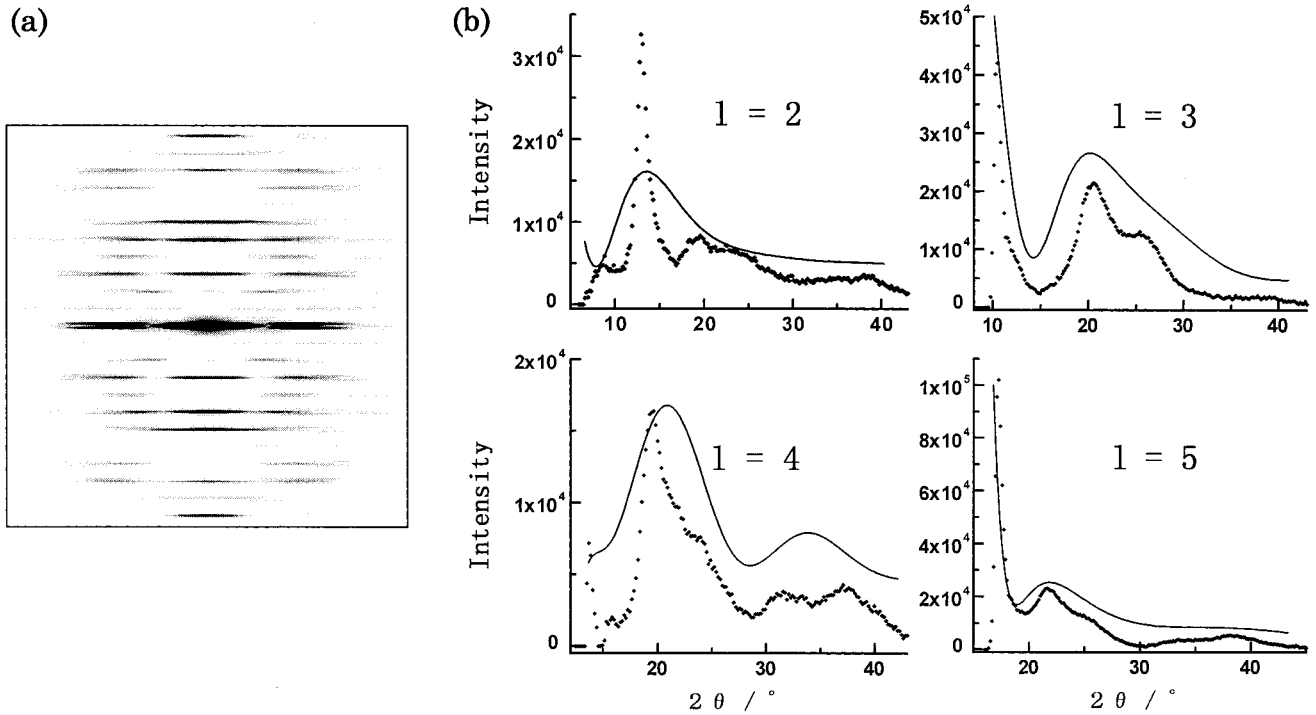

Figure 5. Molecular transform calculated for the uniaxially rotated PBO chain model: (a) 2-dimensional pattern and (b) the profiles along the several layer lines in comparison with the observed data (·).

tions were made also for models II-2 and III-2. The X-ray fiber diagrams were essentially the same as those of models II-1 and III-1 and so are not shown in Figure 4.

Energy Minimization. As stated above, models III-1, III-2, and IV and the related models were found to give relatively good agreement between the calculated and observed diffraction patterns. However, these models might not be always energetically acceptable. Then the energy minimization was carried out for these models. The 16 different types of chain packing were created for each model and the energies were minimized. The X-ray diffraction patterns were calculated for the thus minimized models and averaged. The disorder parameters $\langle \Delta z(x) \rangle$ and the averaged total energies of these structures are

	$\langle \Delta z(a) \rangle$	$\langle \Delta z(b) \rangle$	$\langle \Delta z(1\bar{1}0) \rangle$	energy (kcal/mol monomeric unit)
averaged Model III-1				
before minimization	0.125	0.125	0.033	57.49
after minimization	0.096	0.154	0.016	24.72
averaged Model III-2				
before minimization	0.133	0.117	0.033	57.80
after minimization	0.113	0.138	0.013	24.82
averaged Model IV				
before minimization	0.121	0.131	0.120	101.01
after minimization	0.095	0.133	0.084	25.97

Models III-1 and III-2, obtained after energy minimization, were found to be essentially the same as the energetically minimized model IV as seen from the disorder parameters, in particular, that along the *a* and *b* axes. For these models, the $\langle \Delta z(1\bar{1}0) \rangle$ and $\langle \Delta z(a) \rangle$ become smaller after minimization. In fact, the distribution of the relative height of the adjacent chains in these directions is sharper and can be concentrated to the value *c*/4, as shown in Figure 7, although the degree of this concentration is dependent on the starting model.

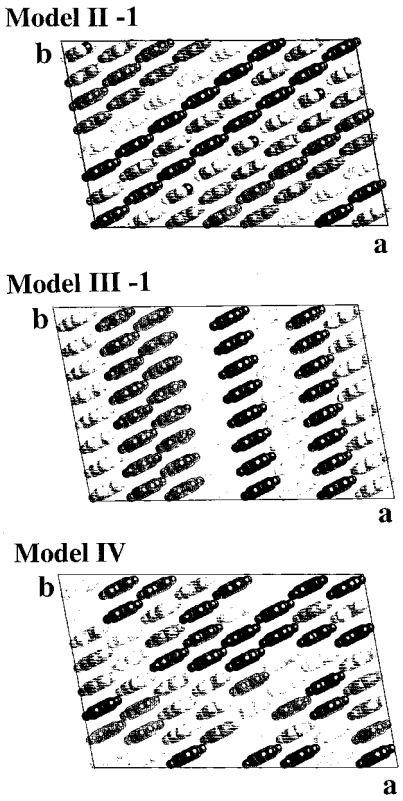

Figure 6. Packing disorder models of PBO crystal. Model II-1: the sheets of chains along the 1$\bar{1}$0 planes are assumed and the relative height of these sheets is randomly disordered (the magnitude of shift is 0−1*c*). Model III-1: the arrays along the *b* axis are assumed for model II-1, and the relative height of these arrays is randomly disordered (the magnitude of shift is 0−0.1*c*). Model IV: all the chains are disordered with respect to the relative height along the chain axis (the magnitude of shift is 0−1*c*). The similar models of II-2 and III-2 were generated starting from the models 0-2 and I-2 shown in Figure 2 but are not reproduced here.

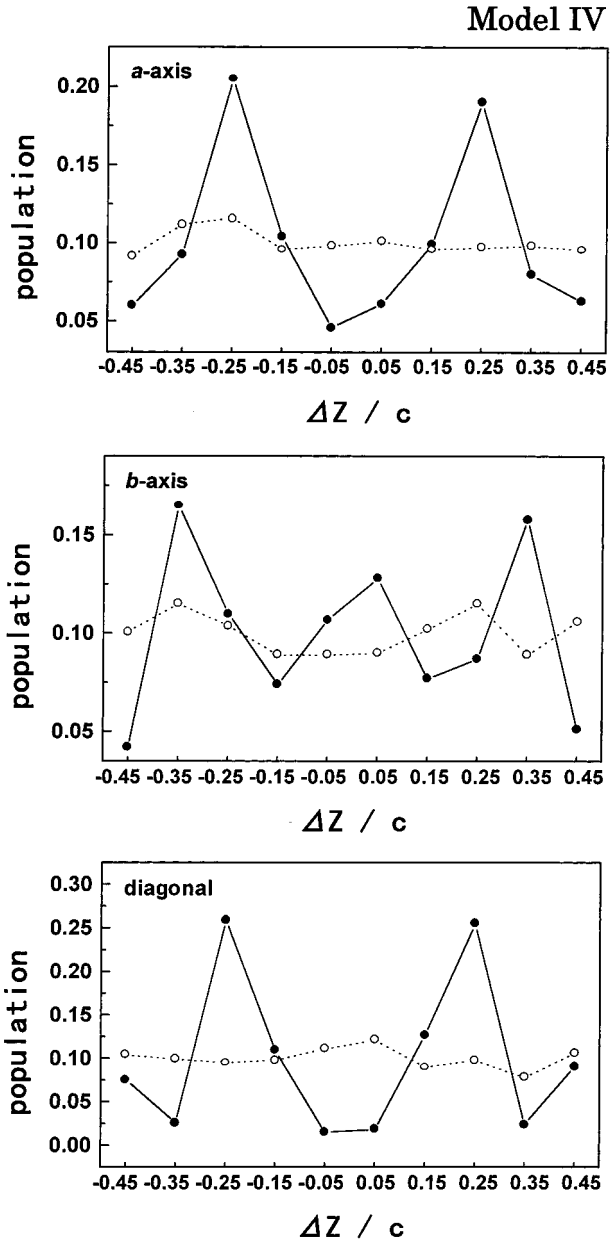

Figure 7. Populations of chains with the various *c*-axial shifts. (from top to bottom) along the *a* axis, along the *b* axis, and along the $1\bar{1}0$ direction. The broken and solid lines are, respectively, before and after the energy minimization.

In this figure the broken lines show the situation before the energy minimization and the populations of the chains having the *c*-axial shifts indicated in the horizontal axis are relatively uniform. This can be said in all the directions of the *a* axis, *b* axis, and $1\bar{1}0$ plane. The solid lines show the results obtained after minimization. As mentioned above, most of the adjacent chains are positioned at the relative height of $\pm c/4$ along the $1\bar{1}0$ direction. This change in the distribution of the relative height of chains seems to come from the energetic stability of the sheet structure assumed along the $1\bar{1}0$ plane.

The X-ray fiber diagrams, averaged for the minimized 16 types of models III-1, III-2, and IV, are compared with the observed ones in Figure 8. In Figure 9 are compared the diffraction profiles of the individual layer lines for model IV as an example. An agreement between the simulated and observed results is appreciably good. When the X-ray fiber pattern of model

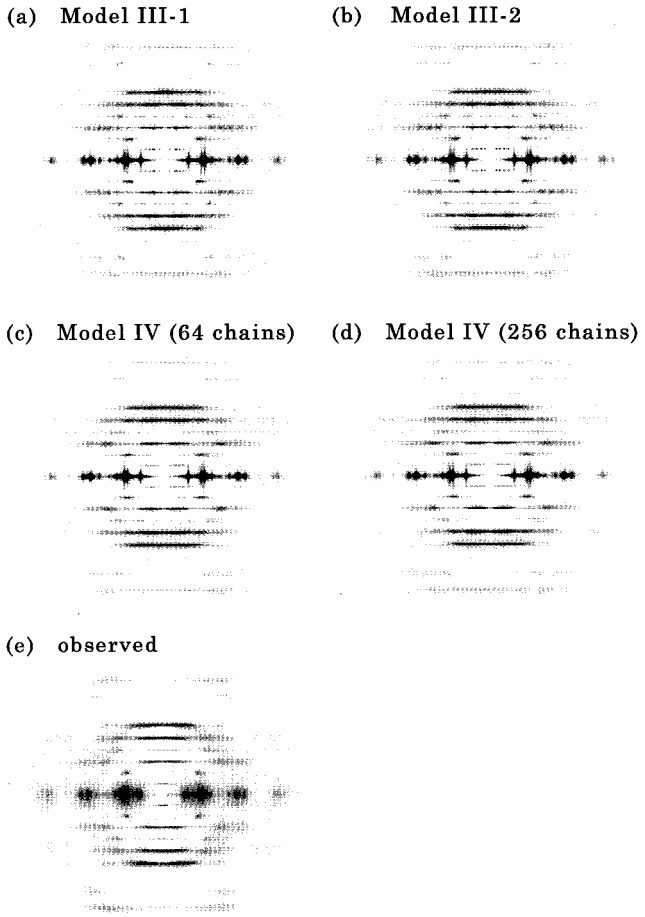

Figure 8. Comparison of the observed X-ray fiber diagram of PBO with the calculated results for the various types of model: (a) model III-1; (b) model III-2; (c) model IV with 64 chains in a cell; (d) model IV with 256 chains in a cell; (e) the observed data. The used X-ray beam is the Mo Kα line.

IV is compared before and after energy minimization [Figures 4e and 8c, respectively], we may notice that the spotlike features of the second layer line become clearer for model IV obtained after the energy minimization. This is considered to come from the energetically more stable sheetlike packing structure of chains along the $1\bar{1}0$ planes with the relative heights of $c/4$ between the adjacent chains. This calculation confirms the prediction by Martin and Thomas[33] that the spotlike reflection of the second layer line should come from the shift of the chains by the $c/4$ height. The models III-1 and III-2 gave essentially the same X-ray profiles with those of model IV. Although these three calculated results are difficult to distinguish from each other, model IV is considered to be the most preferable from the energetic point of view. In fact, both models III-1 and III-2 converged into model IV after energy minimization.

Model IV contains only 64 molecular chains in a repeating cell. Then, to check the effect of the finite cell size, another new type of model IV was constructed, in which the 256 chains were contained in a larger cell and shifted randomly along the chain axis, followed by the energy minimization. The 16 types of this new model were created and the calculated X-ray diffraction patterns were averaged as shown in Figure 8d. In Figure 10 are shown the X-ray diffraction profiles calculated for this model. When Figure 9 is compared with Figure 10, note that the increase of the number of

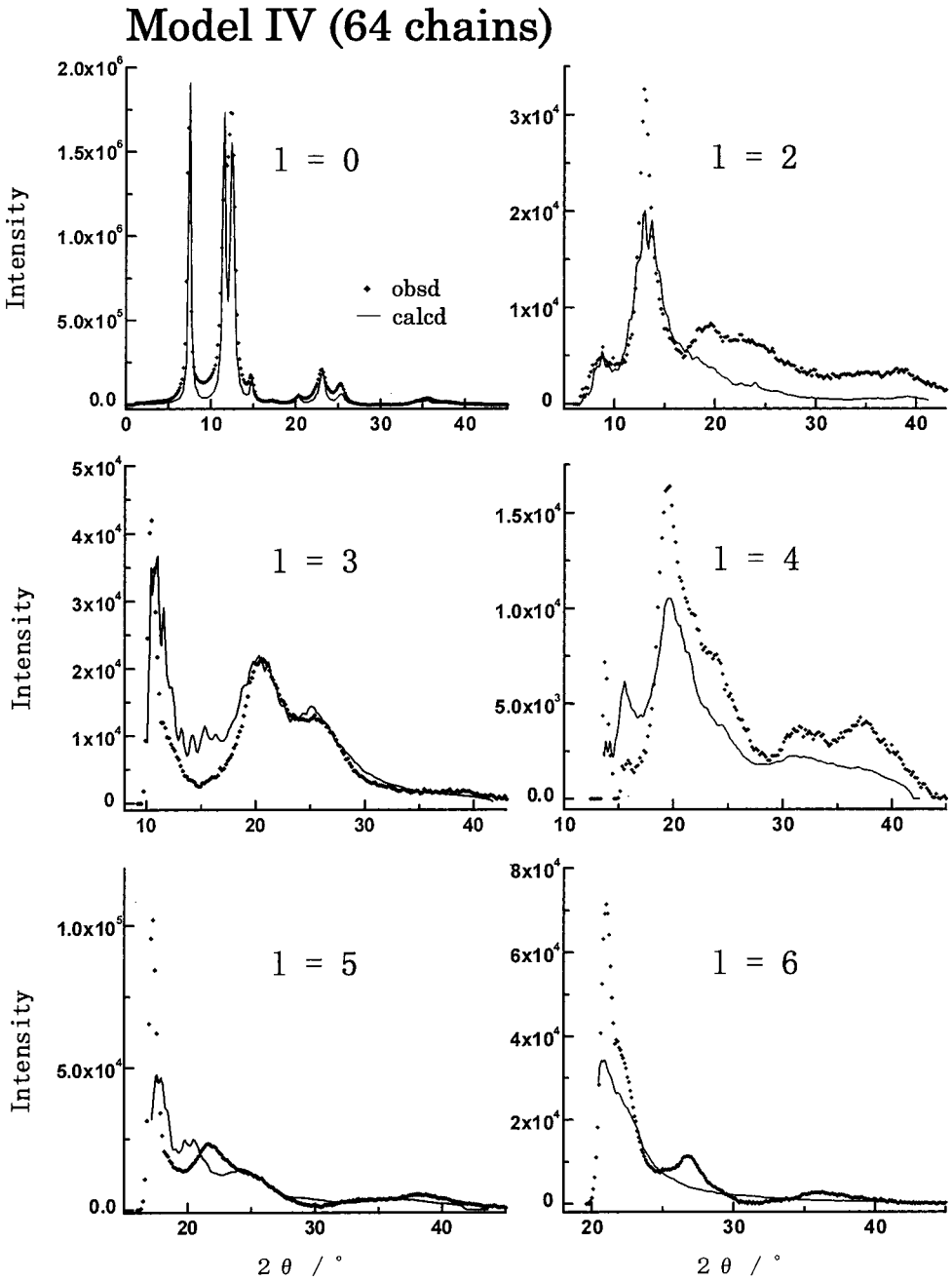

Figure 9. Comparison of the observed X-ray reflectional profiles (●) of PBO fiber with those calculated for model IV with 64 chains in a repeating cell (Figure 6) as indicated by solid lines. The used X-ray beam is the Mo Kα line.

constituent chains from 64 to 256 does not modify the diffraction patterns significantly. We calculate the so-called reliability factor *R* for the X-ray profiles calculated for model IV in comparison with the observed data, where *R* is defined as

$$R\ (\%) = 100\sum|P_i(\text{calc}) - P_i(\text{obsd})|/\sum P_i(\text{obsd})$$

P_i is the profile of the *i*-th layer, and the subtraction between the calculated and observed data was made for all the points of the continuous curves. The summation $\sum$ was made for all the lines of $i = 0-6$. The *R* calculated for the model IV (64 chains) is 19.4% and that for the model IV (256 chains) is 19.0%. The *R* factor is only a measure of the agreement between the observed and calculated profiles along the layer lines. It might be better to calculate the *R* factor not only for the layer lines only but also for all of the points of the 2-dimensional pattern. Anyway, however, the calculated *R* factors indicate the relatively good agreement between the observed and calculated X-ray reflection profiles, implying the reasonableness to assume the model IV obtained after energy minimization to be one of the best candidates to explain the observed X-ray data at the present stage.

Local Order of Chain Packing. As discussed in the preceding section, model IV obtained after energy minimization seems the best structural model of the PBO lattice, where the neighboring chains along the $1\bar{1}0$ planes are shifted by $+c/4$ or $-c/4$ with almost equal probability, and these planes are stacked along the *b* axis at random *c*-axial heights. In other words, the partial registration of chains occurs within the $1\bar{1}0$ planes while the planes themselves are randomly

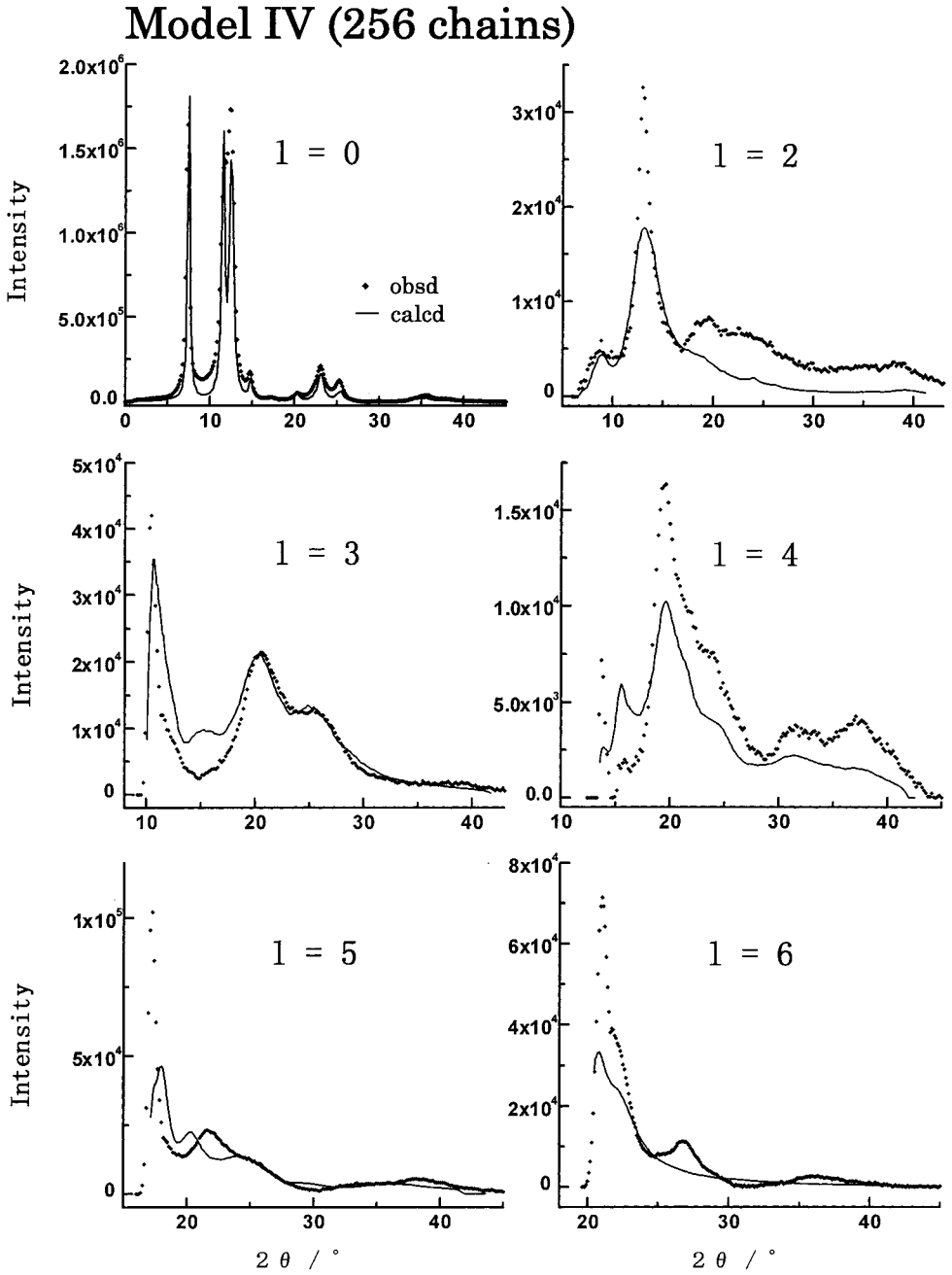

Figure 10. Comparison of the observed X-ray reflectional profiles (●) of PBO fiber with those calculated for model IV with 256 chains in a repeating cell (Figure 6) as indicated by solid lines. The used X-ray beam is the Mo Kα line.

shifted from one another along the chain direction, quite similar structural situation to the poly(*p*-phenylenevinylene) case reported by Granier et al.[46] We searched the domains in which such ordered packing modes are realized to some extent. For example, Figure 11 shows one particular model with a high population of ordered structure. Figure 11a shows the pairs of adjacent chains included in the $1\bar{1}0$ sheet planes, which satisfy the shift of $+c/4$ or $-c/4$ along the chain axis. About 90% or more of the chains are packed with the relative height of $\pm c/4$, reflecting the energetically stable structure of $1\bar{1}0$ sheet structure as pointed out already. (It should be noticed that in Figure 11a, the correlation of chains was investigated only along the $1\bar{1}0$ plane and no attention was paid as to the correlation of chains along the *a* or *b* axis.) Figure 11b shows the groups satisfying the local structures of models 0-1 and I-1 (Figure 2). Different from the packing along the $1\bar{1}0$ planes, the probability of regular structure satisfying the chain packing mode of models 0-1 and I-1 is not so high.

Another Possibility of Disordering. In the present paper we have assumed the disordering of chains occur along the chain axis. As another possible disordering of chain packing we may consider the inversion of chain plane as illustrated in Figure 12. According to the X-ray structure analysis, the low-molecular-weight model compound of PBO

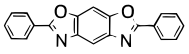

was found to be statistically disordered with respect to the direction of molecular plane.[44,45] That is, the N and O atoms of the heterocyclic ring can be displaced with almost no strain of the crystal lattice. In the polymer

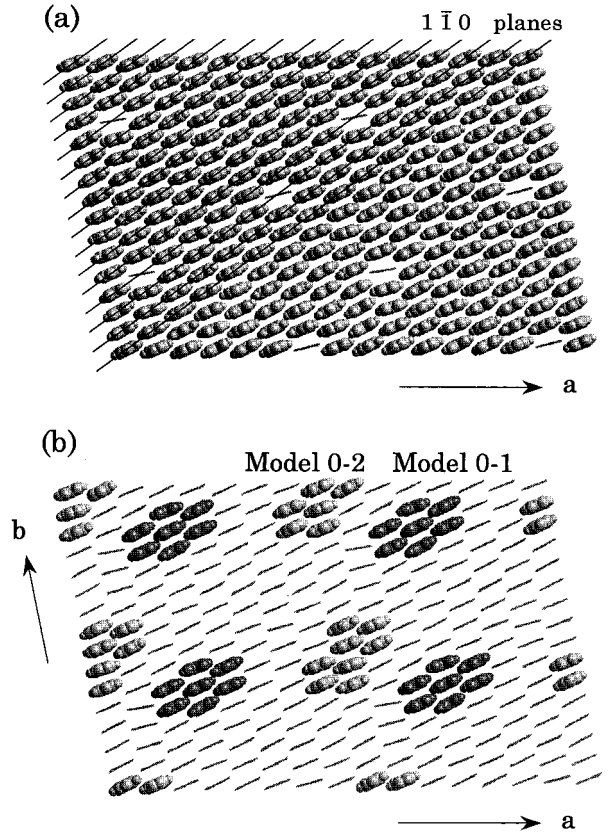

Figure 11. Local structure with regular *c*-axial shift within the disordered PBO crystal (model IV with 256 chains after minimization): (a) the chains satisfying the geometrical relation of $\pm c/4$ shift between the adjacent pairs along the 1$\bar{1}$0 planes; (b) the chains satisfying the geometrical relation of models 0-1 and 0-2.

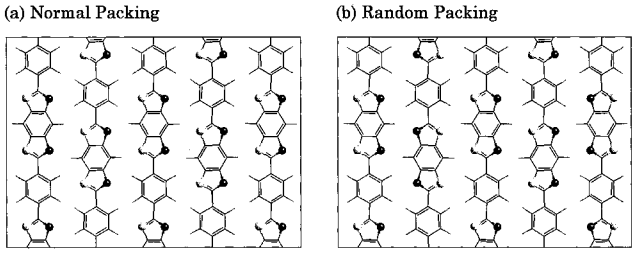

Figure 12. Illustration of packing disorder in PBO crystal as to the N/O atom exchange. The black balls are O atoms and the gray balls are N atoms.

case, also, such type of disordering of chain packing might be possible. In fact, the relative energy of the models with such N/O exchanging disorder does not show any significant difference: 25.97 kcal/mol monomeric unit for model IV and 28.16 kcal/mol monomeric unit for model IV with random N/O exchange. The X-ray diffraction patterns calculated for the two types of model, one being a random exchange of N and O atoms and the other being an alternate arrangement of normal and inverted heterocyclic planes, are also found to be almost the same as those shown in the preceding sections. In this manner, a type of disorder such as statistical exchange of N and O atoms of the heterocyclic rings is also possible in addition to the disorder in the relative height of chains.

Conclusions

In this paper, we proposed the crystal structure of PBO on the basis of the computer simulation of the X-ray diffraction data. Starting from the small unit cell, where models consisted of two or four chains, bigger cell models were proposed in which the disordering with respect to the relative heights of the neighboring chains along the *c* axis was introduced and modified to gain the good agreement between the observed and calculated X-ray diffraction patterns. In these models the chains are assumed to form the sheets extending along the 1$\bar{1}$0 planes and these sheets are shifted more or less with respect to the relative heights along the chain axis. All of these models were found to converge into one model after energy minimization, where the chains in the sheet planes are positioned randomly at the heights of either $+c/4$ or $-c/4$ and the sheets are disordered along the *b* axis with respect to the relative height. The possibility of a random exchange of the N and O atomic positions or the inverted packing of the chain planes is also indicated. Strictly speaking, the structure of PBO fibers may be modified by the heat treatment at different temperatures,[33] but the model proposed in this paper is considered to be quite important as the basic structure for investigating such an annealing effect on the slight change in the packing disorder of chains in the PBO crystal lattice.

Acknowledgment. The authors wish to thank the late Dr. Yoshinori Ogino, director of analysis laboratory of Toyobo Co. Ltd., Dr. Masakatsu Oguchi, director of Polymer Laboratory of Toyobo Co. Ltd., and Dr. Hiroshi Yasuda, director of Fiber Laboratory of Toyobo Co. Ltd., for their kind encouragement in the cooperative research between Osaka University and Toyobo Co. Ltd. This research was supported partly by the Grant-in-Aid for Scientific Research (No. 04403020) from the Ministry of Education, Science, and Culture, Japan.

Note Added in Proof. As seen in Figure 10, for example, the agreement of the simulated X-ray profiles with the observed ones is not very good for the second and sixth layer lines. After the present paper was accepted for publication, we refined furthermore the most plausible structure of PBO (energetically-minimized model IV). A slight change in the relative height of the chains along the 1$\bar{1}$0 and b axes was found to reproduce most of the characteristic features of the observed profiles quite well. In this refined model, on the basis of information about the distribution of chain heights in the energetically-minimized model IV, the relative height of the adjacent chains along the 110 plane was confined to $+0.24c \pm \delta$ and $-0.24c \pm \delta$, not $+0.25c$ and $-0.25c$ as reported in the present paper, and the relative-height of the chains along the b axis was limited to take $\pm (0.39c \pm \delta)$ and $\pm (0.06c \pm \delta)$ at the ratio of 2:1. Here the value 0.02c was assigned to δ. The height of each chain was assigned by using random numbers. The details will be reported in the near future.

References and Notes

(1) Osaheni, J. A.; Jenekhe, S. A.; Burns, A.; Du, G.; Joo, J.; Wang, Z.; Epstein, A. J.; Wang, C. S. *Macromolecules* **1992**, *25*, 5828.

(2) Fawaz, S. A.; Palazotto, A. N.; Wang, C. S. *Polymer* **1992**, *33*, 100.

(3) Hunsaker, M. E.; Price, G. E.; Bai, S. J. *Polymer* **1992**, *33*, 2128.

(4) Fiden, S.; Palazotto, A.; Tsai, C. T.; Kumar, S. *Compos. Sci. Technol.* **1993**, *49*, 291.

(5) Kim, P. K.; Pierini, P.; Wessling, R. *J. Fire Sci.* **1993**, *11*, 296.
(6) Nielsen, C. A.; Pierini, P.; Fuh, S. *J. Fire Sci.* **1993**, *11*, 156.
(7) Lee, C. Y.; Santhosh, U. *Polym. Eng. Sci.* **1993**, *33*, 907.
(8) Connolly, J. W.; Dudis, D. S. *Polymer* **1993**, *34*, 1477.
(9) Jones, M. C. G.; Martin, D. C. *Macromolecules* **1995**, *28*, 6161.
(10) Hirahira, H.; Yabuki, K.; *Kino Zairyo* **1996**, *16*, 5.
(11) Yabuki, K. *Sen'i Gakkaishi* **1996**, *52*, 143.
(12) Natsuhara, T. *Kako Gijutsu* **1996**, *31*, 566.
(13) Lenhart, P. G.; Adams, W. W. *Mater. Res. Soc. Symp. Proc.* **1989**, *134*, 329.
(14) Tashiro, K.; Kobayashi, M. *Macromolecules* **1991**, *24*, 3706.
(15) Wierschke, S. G.; Shoemaker, J. R.; Haaland, P. D.; Pachter, R.; Adams, W. W. *Polymer* **1992**, *33*, 3357.
(16) Nakamae, K.; Nishino, T.; Matsui, Y.; Goto, Y.; Nakura, M. *Polym. Prepr. Jpn.* **1995**, *44*, 2061.
(17) Adams, W. W.; Kumar, S.; Shimamura, K. *Polym. Commun.* **1989**, *30*, 285.
(18) Krause, S. J.; Haddock, T. B.; Vezie, D. L.; Lenhert, P. G.; Hwang, W.-F.; Price, G. E.; Helminiak, T. E.; O'Brien, J. F.; Adams, W. W. *Polymer* **1988**, *29*, 1354.
(19) Young, R. J.; Day, R. J.; Zakikihani, M. *J. Mater. Sci.* **1990**, *25*, 127.
(20) Bai, S. J.; Price, G. E. *Polymer* **1992**, *33*, 2136.
(21) Zhang, R.; Mattice, W. L. *Macromolecules* **1992**, *25*, 4937.
(22) Nolan, S. J.; Mills, M. J.; Radler, M. J.; Broomall, C. F.; Bubeck, R. A.; Landes, B. G.; Rudolf, P. R. *Mater. Res. Soc. Symp. Proc.* **1993**, *305*, 111.
(23) Roitman, D. B.; McAdon, M. *Macromolecules* **1993**, *26*, 4381.
(24) Bai, S. J. *J. Polym. Sci., Part B: Polym. Phys.* **1994**, *32*, 2575.
(25) Kumar, S.; Warner, S.; Grubb, D. T.; Adams, W. W. *Polymer* **1994**, *35*, 5408.
(26) Mehta, V. R.; Kumar, S. *J. Mater. Sci.* **1994**, *29*, 3658.
(27) Martin, D. C.; Thomas, E. L. *Polymer* **1995**, *36*, 1743.
(28) Nolan, S. J.; Broomall, C. F. *Rev. Sci. Instrum.* **1995**, *66*, 2652.
(29) Chau, C. C.; Blackson, J.; Im, J. *Polymer* **1995**, *36*, 2511.
(30) Sherman, B. J.; Sen, S.; Galiatsatos, V. *Polymer* **1996**, *37*, 1759.
(31) Choe, E. W.; Kim, S. N. *Macromolecules* **1981**, *14*, 920.
(32) Fratini, A. V.; Lenhert, P. G.; Resch, T. J.; Adams, W. W. *Mater. Res. Soc. Symp. Proc.* **1989**, *134*, 431.
(33) Martin, D. C.; Thomas, E. L. *Macromolecules* **1991**, *24*, 2450.
(34) Bhaumik, D.; Welsh, W. J.; Jaffe, H. H.; Mark, J. E. *Macromolecules* **1981**, *14*, 951.
(35) Martin, D. C. *Macromolecules* **1992**, *25*, 5171.
(36) Welsh, W. J.; Yang, Y. *Comput. Polym. Sci.* **1991**, *1*, 139.
(37) Farmer, B. L.; Chapman, B. R.; Dudis, D. S.; Adams, W. W. *Polymer* **1993**, *34*, 1588.
(38) Connolly, J. W.; Dudis, D. S. *Mater. Res. Soc. Symp. Proc.* **1993**, *291*, 591.
(39) Shaffer, A. A.; Wierschke, S. G. *J. Comput. Chem.* **1993**, *14*, 75.
(40) Karna, S. P.; Keshari, V.; Prasad, P. N. *Chem. Phys. Lett.* **1995**, *234*, 390.
(41) Tashiro, K.; Asanaga, H.; Ishino, K.; Tazaki, R.; Kobayashi, M. *J. Polym. Sci. B: Polym. Phys.* **1997**, *35*, 1677.
(42) Tashiro, K. Reports on Research Project, Grant-in-Aid for Developmental Scientific Research (B). The Ministry of Education, Science, and Culture, Japan, March 1994.
(43) Tashiro, K. Reports on Research Project, Grant-in-Aid for Developmental Scientific Research (A). The Ministry of Education, Science, and Culture, Japan, March 1997.
(44) Tashiro, K.; Ishino, K.; Abe, Y.; Kobayashi, M. *Rep. Prog. Polym. Phys. Jpn.* **1996**, *39*, 329.
(45) Wellman, M. W.; Adams, W. W.; Wiff, D. R.; Fratini, A. V. Technical Reports. AFML-TR-79-4184, Part I; 1979.
(46) Granier, T.; Thomas, E. L.; Karasz, E. *J. Polym. Sci.: Part B: Polym. Phys.* **1989**, *27*, 469.
(47) Suehiro, K.; Chatani, Y.; Tadokoro, H. *Polym. J.* **1975**, *7*, 352.
(48) Mayo, S. L.; Olafson, B. D.; Goddard, W. A. *J. Phys. Chem.* **1990**, *94*, 8897.
(49) Gasteiger, J.; Marsili, M. *Tetrahedron* **1980**, *36*, 3219.

MA980113R